Int J Thermophys (2009) 30:1400–1410
DOI 10.1007/s10765-009-0585-3

Structure Sensitive Properties of Liquid Al–Si Alloys

V. Sklyarchuk · Yu. Plevachuk · A. Yakymovych · S. Eckert · G. Gerbeth · K. Eigenfeld

Received: 17 October 2008 / Accepted: 20 April 2009 / Published online: 9 May 2009

Abstract Development and application of new expedient aluminum-based light alloys are a key issue in current material science. In this study measurements are presented for the thermophysical properties of liquid Al–7Si, AlSi7Mg, and AlSi8Cu3 (mass%) alloys, which are the most utilized casting alloys in the aluminum industry. Experimental data with respect to the density, viscosity, and the electrical and thermal conductivities have been determined in a wide temperature range, and corresponding fit relations have been derived. Comparisons with already published data and scaling relations available in the literature are given.

Keywords Al–Si alloys · Density · Electrical conductivity · Thermal conductivity · Viscosity

1 Introduction

An increasing demand for lighter cars and airplanes provokes an intensive research in the field of high-strength light metals. Aluminum casting alloys are essential for the automotive, aerospace, and engineering industries. Such alloys mainly contain Si,

V. Sklyarchuk · Yu. Plevachuk (✉) · A. Yakymovych
Department of Metal Physics, Ivan Franko National University,
Lviv, Ukraine
e-mail: plevachuk@mail.lviv.ua

S. Eckert · G. Gerbeth
MHD Department, Forschungszentrum Dresden-Rossendorf,
Dresden, Germany

K. Eigenfeld
Foundry Institute, TU Bergakademie Freiberg, Freiberg, Germany

Cu, and Mg as the major alloying elements. Copper and magnesium strengthen the alloy matrix and improve the mechanical properties and machinability [1,2]. Silicon doping reduces the thermal expansion coefficient, increases corrosion and wear resistance, and improves the casting and machining characteristics of the alloy [3]. Therefore, near-eutectic Al–Si alloys are widely used in automotive applications, especially for the piston fabrication. Due to their excellent castability, Al–Si alloys are mainly used for highly complex and thin-walled castings. Moreover, these alloys feature a high strength-to-weight ratio.

A well-directed adjustment of the physical properties of Al–Si alloys in the solid state also requires studies of the liquid metal. A knowledge of thermophysical properties in the liquid state is of crucial importance to optimize technological equipment and operations, such as solidification in casting processes or powder production by atomization. Considerable effort has been made to set-up numerical models for calculation of fluid flow, heat and mass transfer, and solidification in casting processes. These numerical models are important tools for a better understanding of the physics of solidification and to improve the quality of products. However, predictions of the numerical simulations concerning quantities such as the time-dependent temperature profiles and concentration profiles, the extension and the consistence of the mushy zone, solidification rates, or the morphology of the resulting microstructure are extremely sensitive with respect to the thermo-physical properties [4].

The density is directly related to the atomic structure and potential short-range order of the liquid. On the other hand, it is a fundamental quantity for all technological applications, since it determines essential dimensionless parameters characterizing fluid flow, such as the Reynolds number or the Rayleigh number. A knowledge of the viscosity is of particular importance for considering the relationship between melt convection and solidification. The thermal conductivity plays an important role for heat transfer, especially in the mushy zone during recalescence. The application of magnetic fields provides an attractive tool for electromagnetic flow control in casting operations. The respective electromagnetic force scales with the electrical conductivity of the metallic alloy. Furthermore, reliable information about the structural heterogeneity of the melt can, in principle, be obtained from studies considering the temperature dependence of the electrical conductivity and the viscosity [5,6].

Our investigations are restricted to hypoeutectic Al–Si alloys with Cu and Mg admixtures, namely, the Al–7Si alloy and the commercially used cast alloys AlSi7Mg (A356) and AlSi8Cu3 (226). The thermo-physical properties have been determined for the density, dynamic viscosity, thermoelectric power, and electrical and thermal conductivities. The measurements cover a wide temperature range above the liquidus temperature.

2 Experimental Methods

The Al–7Si alloy has been prepared from 99.99 mass% Al and 99.999 mass% Si according to the designated composition. AlSi7Mg and AlSi8Cu3 are commercial

Table 1 Concentration of the alloying elements in the cast alloys AlSi7Mg and AlSi8Cu3 (in mass%)

Alloy (mass%)	Si	Fe	Cu	Mn	Mg	Ni	Zn	Ti
AlSi7Mg	6.5–7.5	0.18	0.05	0.1	0.25–0.45	–	0.07	0.001–0.2
AlSi8Cu3	7.5–9.5	0.7	2.0–3.5	0.15–0.65	0.15–0.55	0.35	1.2	0.2

cast alloys which were provided by the Foundry Institute of the TU Bergakademie Freiberg. The respective compositions are given in Table 1.

2.1 Density

The density, $\rho(T)$, was measured using the "large-drop" method. This method is a modification of the sessile-drop method and allows for overcoming problems connected with a large sessile drop asymmetry [7,8]. A circular crucible, which has its upper circumferential edge chamfered to an acute angle, is overfilled with fluid, so that an axisymmetric meniscus, with a diameter exceeding the diameter of the crucible is produced standing above the rim. In the final analysis, this construction reduces the error of the drop volume determination. The latter introduces a main error in the density determination, while a mass determination error is negligibly small. The experiments were performed in an atmosphere of 90 % Ar + 10 % H_2 after initially pumping out the working volume of the chamber in order to avoid sample oxidation. The temperature has been measured with WRe5/20 thermocouple placed near the specimen and was kept constant within 1 K. Density measurements of the selected alloys in the liquid phase pose experimental difficulties because of a large difference in the melting temperatures of the constituents. Aluminum evaporates extensively at elevated temperatures leading to a shift in the sample composition. Therefore, each sample was measured several times in order to get reliable values of the density. In addition, the samples were weighed before and after the experiments. If a sample lost more than 0.1 % of its initial mass, the measurements were rejected. The total error for the density measurements is estimated to be about 3 %.

2.2 Viscosity

The measurements of the viscosity were carried out using a computer-controlled oscillating-cup viscometer [9]. The temperature dependence of the dynamic viscosity, $\eta(T)$, has been calculated from the corresponding logarithmic decrement and the periodic time of the oscillations using the modified Roscoe equation. The experiments were performed in a helium atmosphere under a negligible excess pressure of about 0.02 MPa to 0.03 MPa. Each sample has been weighed before and after the measurements, and no loss of mass has been observed. Cylindrical boron nitride crucibles with an internal diameter of 14 mm were used. The temperature has been measured with a WRe-5/20 thermocouple located just below the crucible. The viscosity data were obtained with an uncertainty of about 3 %.

2.3 Electrical Conductivity and Thermoelectric Power

The electrical conductivity, $\sigma(T)$, and thermoelectric power, $S(T)$, were measured by a contact method in accordance with the four-point scheme. The experiments were performed in an argon atmosphere. Graphite electrodes for current and potential measurements were placed in the wall of the vertical cylindrical BN-ceramic measuring cell along its vertical axis. The potential electrodes were provided with thermocouples for temperature measurements. Single thermoelectrodes of these thermocouples were used for electrical conductivity determination. The melt temperature was determined by WRe5/20 thermocouples in close contact with the liquid. The resultant error of the electrical conductivity measurements is about 2 %, and 5 % for the thermoelectric power determination. For further details of this method and its experimental realization, we refer the reader to [10].

2.4 Thermal Conductivity

An experimental arrangement based on the steady-state concentric cylinder method was used for thermal-conductivity measurements [11]. The apparatus comprises two coaxial cylinders (stainless steel, BN, or graphite) separated by a gap, into which the melt is poured. A central hole is drilled in the inner cylinder for an internal heater made of a molybdenum wire, wound on an alumina form. The inner heater is used for producing the necessary temperature gradient in the investigated melt layer. The cell is closed by a BN cover, which is sealed with a special compound based on a finely dispersed BN powder. The outer three-section furnace is made of molybdenum wire wound on a BN form. The outer heater produces an overall temperature level, and its upper and lower sections permit regulation of the temperature field over the height of the apparatus. Tungsten–rhenium WR5/20 thermocouples were used in the experiments. Two thermocouples placed in the body of the inner cylinder allow the examination of the temperature distribution over the radius of the apparatus. The coefficient of thermal conductivity, $\lambda(T)$, can be calculated from the formula for the heat transfer in a cylindrical layer. The design of the apparatus assures maximum reduction of heat leakage and convection. The resultant uncertainty of thermal conductivity measurements is about 7 %.

3 Results and Discussion

3.1 Density of Al–Si Alloys

The density of Al–7Si, AlSi7Mg, and AlSi8Cu3 liquid alloys was measured in a wide temperature range above the liquidus temperature. The measured values of the density for the alloys studied are presented in Fig. 1. The temperature dependence of the density in the temperature interval investigated can be well fitted with linear functions for all compositions:

$$\rho(T) = \rho_{\mathrm{L}} + \rho_{\mathrm{T}}(T - T_{\mathrm{L}}), \tag{1}$$

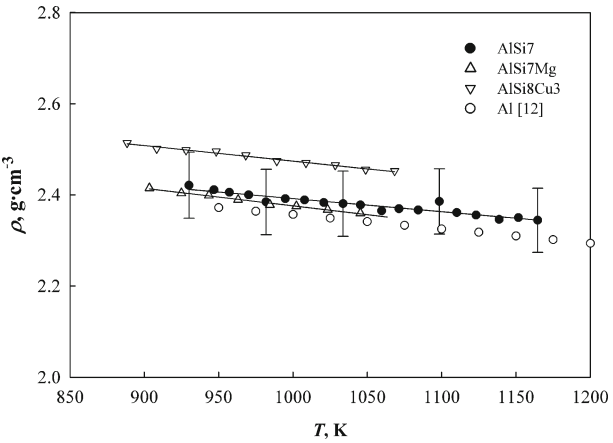

Fig. 1 Temperature dependence of the density for liquid Al–Si alloys. Lines are linear fits to the experimental data (see Table 2 for details)

Table 2 Parameters of the linear fits $\rho(T) = \rho_L + \rho_T (T - T_L)$ to the measured density for liquid Al–Si alloys

Alloy (mass%)	T_L (K)	ρ_L(g · cm^{-3})	ρ_T (10^{-4}g · cm^{-3} · K^{-1})
AlSi7	908	2.42	−2.87
AlSi7Mg	873	2.42	−3.86
AlSi8Cu3	836	2.51	−3.41

where ρ_L is the density at the liquidus temperature T_L, and ρ_T is the thermal coefficient of the density. The experimental data are plotted in Fig. 1. The parameters ρ_L, ρ_T are obtained by fitting these data and are listed in Table 2 together with the liquidus temperature T_L. The density results are compared to the reference data of pure aluminum [12]. It can be seen that the density increases with an increase of the copper and silicon content, while the addition of magnesium has practically no influence on the density value.

3.2 Viscosity of Al–Si Alloys

The viscosity data for Al and the Al–7Si, AlSi7Mg, and AlSi8Cu3 liquid alloys are plotted in Fig. 2 together with data published for pure aluminum [12]. It should be noted that among different structure-sensitive properties the viscosity of pure liquid aluminum reveals the largest scatter of values, e.g., from 1.2 mPa · s to 1.4 mPa · s at the melting point [12–16]. The present viscosity values obtained for Al are very close to the data reported by Assael et al. [12].

The temperature dependence of the viscosity, η, (in mPa · s) is well described by the Arrhenius equation:

$$\eta = \eta_0 \exp\left(\frac{E}{RT}\right) \tag{2}$$

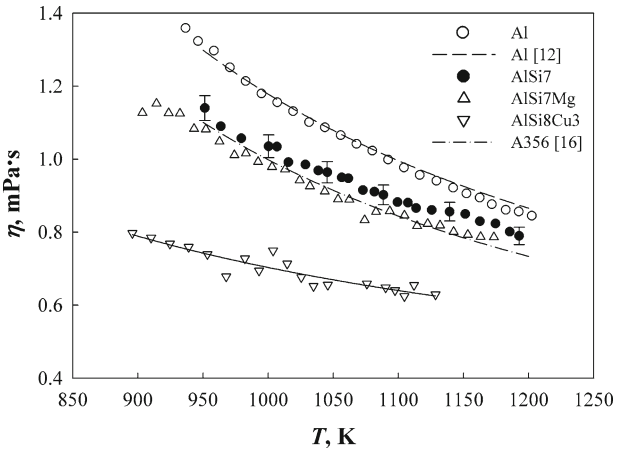

Fig. 2 Temperature dependence of the viscosity for liquid Al–Si alloys. For AlSi8Cu3 the solid line reflects the Arrhenius fit to the experimental data (see Table 3 for details)

Table 3 Fitting parameters of $\eta = \eta_0 \exp(E/RT)$ to the measured viscosity for liquid Al and Al–Si alloys

Alloy (mass%)	η_0 (mPa · s)	E (J · mol^{-1})
Al	0.16	16626
AlSi7	0.206	13385
AlSi7Mg	0.193	13517
AlSi8Cu3	0.25	8609

where R is the universal gas constant (J · mol^{-1} · K^{-1}), T is the absolute temperature (K), E is the activation energy (J · mol^{-1}), and η_0 is a constant (mPa · s). The fitting curve is shown in Fig. 2 only for the AlSi8Cu3 alloy and is omitted for other compositions, for the sake of clarity. The fitted numerical parameters corresponding to different alloys are given in Table 3.

As seen from Fig. 2, the viscosity and the activation energy of liquid aluminum decrease with admixtures of silicon. The viscosity curves of liquid AlSi7 and AlSi7Mg alloys are in close agreement with earlier reported data for the commercial A356 alloy measured by the same oscillating-cup method [16]. These results confirm the assumption that small magnesium amounts have practically no influence on the viscosity [17].

The lower viscosity values of AlSi8Cu3 could be mainly affected by higher silicon content. Such a tendency is already known from previous studies [18,19]; however, the authors provided no reasonable explanation for that behavior. The Al–Si system phase diagram is of a simple eutectic type [20]. Structure investigations revealed predominance of clusters, composed mainly of the atoms of different types [21,22]. These clusters, whose lifetime prevails over the lifetime of clusters containing only one-type atoms, could be considered as self-dependent units of the viscous flow. The valence electrons participate in the formation of inner bonds. As a result, an

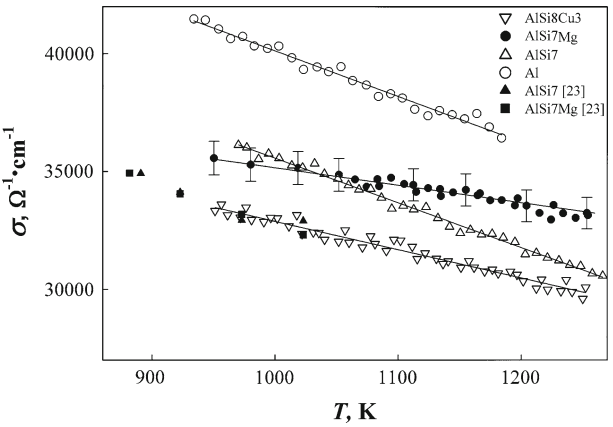

Fig. 3 Temperature dependence of the electrical conductivity for liquid Al and AlSi7, AlSi7Mg, and AlSi8Cu3 liquid alloys. Lines are linear fits to the experimental data (see Table 4 for details)

Table 4 Parameters of the linear fits $\sigma = \sigma_0 + \mathrm{d}\sigma/\mathrm{d}T\,(T - T_\mathrm{L})$ to the measured electrical conductivity for liquid Al and Al–Si alloys

Alloy (mass%)	T_L (K)	σ_0 ($\Omega^{-1} \cdot \mathrm{cm}^{-1}$)	$\mathrm{d}\sigma/\mathrm{d}T$ ($\Omega^{-1} \cdot \mathrm{cm}^{-1} \cdot \mathrm{K}^{-1}$)
Al	933	41400	−19.36
AlSi7	908	37310	−18.9
AlSi7Mg	873	36097	−7.4
AlSi8Cu3	836	34850	−11.99

interaction between the Al–Si clusters and surrounding atoms becomes weaker. As mutual particle displacements are directed towards the weakest bonds, both the viscosity and the activation energy decrease.

3.3 Electrical Conductivity and Thermoelectric Power of Al–Si Alloys

The electrical conductivity is displayed in Fig. 3 as a function of the temperature, $\sigma(T)$. Measured values are presented for Al–7Si, AlSi7Mg, and AlSi8Cu3 melts together with data for pure Al for comparison. The $\sigma(T)$ dependence for all the melts is well described by the linear equation:

$$\sigma = \sigma_0 + \frac{\mathrm{d}\sigma}{\mathrm{d}T} \times (T - T_\mathrm{L}) \tag{3}$$

where σ_0 is the electrical conductivity (in $\Omega^{-1} \cdot \mathrm{cm}^{-1}$) at the melting point and $\mathrm{d}\sigma/\mathrm{d}T$ is the temperature coefficient of conductivity. The electrical conductivity of all melts considered here decreases gradually with heating according to Eq. 3. The parameters of the linear fits are given in Table 4.

It was revealed that small amounts of silicon, copper, and magnesium decrease the absolute conductivity value as compared with pure Al. The absolute $\sigma(T)$ values for the AlSi7Mg alloy are found to be less than that for the binary Al–7Si. The lowest

$\sigma(T)$ values were measured for the AlSi8Cu3 alloy. The lowest temperature coefficient of conductivity has been observed for the AlSi7Mg alloy. The present $\sigma(T)$ data for AlSi7 and AlSi7Mg are slightly higher than the values reported in [23] (see Fig. 3). The difference could be explained by the deviation in the sample compositions as well as by experimental uncertainties.

It is generally assumed that an addition of admixtures decreases the electrical conductivity. The conductivity increment $\Delta\sigma_\mathrm{i}$ can be determined from the following equation:

$$\Delta\sigma_\mathrm{i}^{-1} = N_\mathrm{i}\frac{m\upsilon_\mathrm{F}}{e^2}\Sigma_\mathrm{i} \tag{4}$$

where Σ_i is the scattering cross section of the conducting electrons at the admixture particles, N_i is the atomic fraction of these impurities, m is the electron mass, e is the electron charge, and υ_F is the electron velocity at the Fermi level [24]. In a simplest case, when the impurity scattering does not depend on other scattering mechanisms, $\Delta\sigma_\mathrm{i}$ is independent of the temperature. However, Eq. 4 describes the decrease of the electrical conductivity only roughly. A better approximation can be attained by using the partial wave method and the Friedel sum rule [25]. Considering approximated potentials in the scattering cross section, the following expression is valid:

$$\Delta\sigma_\mathrm{i}^{-1} = N_\mathrm{i}[a + b(\Delta Z)^2] \tag{5}$$

where a and b depend on the host metal and the row of the Periodic Table to which the solute belongs. The variable ΔZ is the difference between valences of an impurity and a solvent. Such a relationship, the so-called Linde rule, is valid for a number of binary liquid alloys. The behavior of the electrical conductivity in multicomponent systems is usually more complicated.

The electrical conductivity of the liquid alloy in the free electron approximation is expressed as [26]

$$\sigma = \frac{n_\mathrm{e}e^2}{\hbar k_\mathrm{f}}L \tag{6}$$

where $\hbar$ is the Planck constant, n_e is the electron density, and L is the mean free path of conduction electrons. The admixtures inevitably decrease the electron mean free path, which leads, in turn, to a decrease in the conductivity.

The experimental temperature dependence of the thermoelectric power, $S(T)$, is presented in Fig. 4 for the considered alloys. The thermoelectric power of all liquid alloys remains negative in the investigated temperature range. The absolute values increase practically linearly from $-1\,\mu\mathrm{V}\cdot\mathrm{K}^{-1}$ to $-3\,\mu\mathrm{V}\cdot\mathrm{K}^{-1}$. The data for AlSi7 and AlSi7Mg almost coincide, while the absolute $S(T)$ values of AlSi8Cu3 are lower. Such thermoelectric power behavior is typical for metal systems. To the best of our knowledge, such $S(T)$ studies were carried out for the first time for Al–Si alloys.

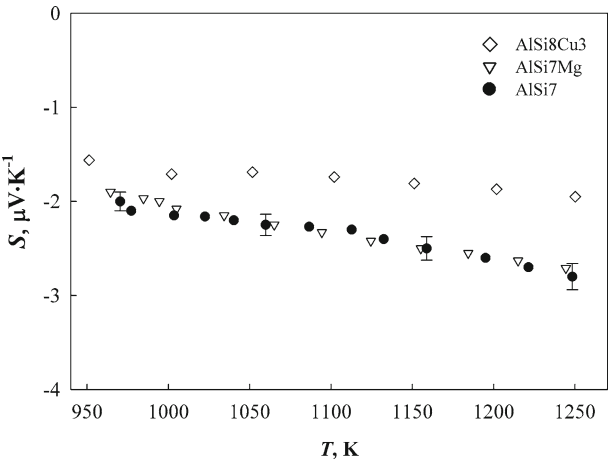

Fig. 4 Temperature dependence of the thermoelectric power for AlSi7, AlSi7Mg, and AlSi8Cu3 liquid alloys

Table 5 Parameters of the linear fits $\lambda = \lambda_0 + b(T - T_L)$ to the measured thermal conductivity for liquid Al–Si alloys

Alloy (mass%)	T_L (K)	λ_0 ($W \cdot m^{-1} \cdot K^{-1}$)	b ($W \cdot m^{-1} \cdot K^{-2}$)
AlSi7	908	87.1	0.027
AlSi7Mg	873	88.3	0.037
AlSi8Cu3	836	76.2	0.046

3.4 Thermal Conductivity of Al–Si Alloys

The temperature dependence of the thermal conductivity, $\lambda(T)$, was measured in the temperature range from the melting point up to 1,250 K. The $\lambda(T)$ dependence could be well described by the linear equation:

$$\lambda = \lambda_0 + b(T - T_L) \tag{7}$$

where λ_0 is the thermal conductivity (in $W \cdot m^{-1} \cdot K^{-1}$) at the melting point and b is the temperature coefficient of the thermal conductivity. The parameters of the linear fits are specified in Table 5. The thermal conductivity increases with heating for all investigated alloys according to Eq. 7. The absolute thermal conductivity values as well as their temperature dependence suggest a prevalence of conduction electrons in the heat transfer. These values also prove rather strong gas degeneracy [27]. In this case the Wiedemann–Franz–Lorenz law can be used and the Lorenz number can be determined. The calculations revealed that the Lorenz number is constant in the investigated temperature range and is very close to its theoretical (Sommerfeld-) value of $2.445 \times 10^{-8}\,W \cdot \Omega \cdot K^{-2}$.

As shown in Fig. 5, the present data are consistent with thermal-conductivity results reported in [23], which were calculated from the electrical conductivity.

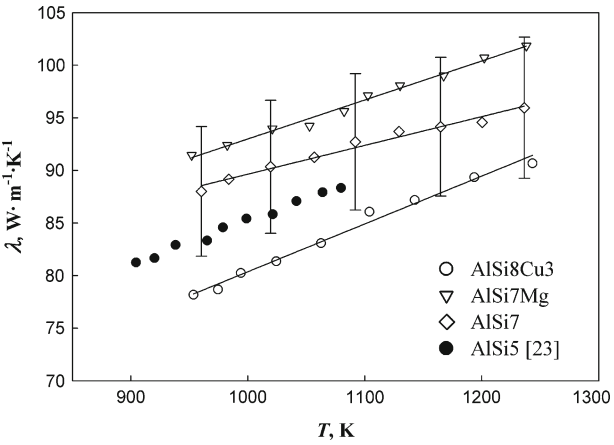

Fig. 5 Temperature dependence of thermal conductivity for liquid AlSi7, AlSi7Mg, and AlSi8Cu3 alloys. Lines are linear fits to the experimental data (see Table 5 for details)

4 Conclusions

Several thermophysical properties of liquid hypoeutectic Al–Si alloys have been measured in the temperature range from the melting point up to 1,250 K. Corresponding fit relations have been derived for the density (see Eq. 1), the dynamic viscosity (see Eq. 2), the electrical conductivity (Eq. 3) and the thermal conductivity (see Eq. 7). The growing silicon content results in a gradual increase in the density and a decrease in the dynamic viscosity of aluminum. Admixtures of Si, Cu, and Mg result in a decrease of the electrical conductivity of aluminum. This finding is explained by a decrease of the electron mean free path. The thermoelectric power is negative and typical for metal systems. The experimental thermal conductivity agrees with calculated data according to the Wiedemann–Franz–Lorenz law, while the Lorenz number is constant in the investigated temperature range.

Acknowledgment This work was financially supported by Deutsche Forschungsgemeinschaft (DFG) in form of the collaborative research centre SFB 609 "Electromagnetic Flow Control in Metallurgy, Crystal Growth and Electrochemistry."

References

1. P. Ouellet, F.H. Samuel, J. Mater. Sci. **34**, 4671 (1999)
2. P.N. Crepeau, S.D. Antolovich, J.A. Worden, AFS Trans. **98**, 813 (1990)
3. M.M. Haque, A. Sharif, J. Mater. Process. Technol. **118**, 69 (2001)
4. A. Ludwig, P. Quested, G. Neuer, Adv. Eng. Mater. **3**, 11 (2001)
5. U. Dahlborg, M. Calvo-Dahlborg, P.S. Popel, V.E. Sidorov, Eur. Phys. J. **B14**, 639 (2000)
6. S.I. Mudry, V.M. Sklyarchuk, Yu.O. Plevachuk, I.I. Shtablavyi, Inorg. Mater. **44**, 129 (2008)
7. Yu.V. Naidich, V.N. Eremenko, Fiz. Met. Metalloved. **11**, 883 (1961)
8. V.M. Glazov, M. Wobst, V.I. Timoshenko, *Investigation Methods of the Properties of Liquid Metals and Semiconductors* (Metallurgiya, Moscow, 1989), pp. 139–149
9. S. Mudry, V. Sklyarchuk, A. Yakymovych, J. Phys. Studies **12**, 1601 (2008)

10. Yu. Plevachuk, V. Sklyarchuk, Meas. Sci. Technol. **12**, 23 (2001)
11. V. Sklyarchuk, Y. Plevachuk, Meas. Sci. Technol. **16**, 467 (2005)
12. M.J. Assael, K. Kakosimos, R.M. Banish, J. Brillo, I. Egry, R. Brooks, P.N. Quested, K.C. Mills, A. Nagashima, Y. Sato, W.A. Wakeham, J. Phys. Chem. Ref. Data. **35**, 285 (2006)
13. A.T. Dinsdale, P.N. Quested, J. Mater. Sci. **39**, 7221 (2004)
14. T. Iida, Y. Shiraishi, in *Handbook of Physico-chemical Properties at High Temperatures*, chap. 4 Viscosity, ed. by Y. Kawai, Y. Shirashi (The Iron and Steel Institute of Japan (ISIJ), Tokyo, 1988)
15. L. Battezzati, A.L. Greer, Acta Metall. **37**, 1791 (1989)
16. D. Wang, R.A. Overfelt, Int. J. Thermophys. **23**, 1063 (2002)
17. Y. Wang, Y. Wu, X. Bian, Chinese Sci. Bull. **52**, 1441 (2007)
18. L.A. Koledov, A.P. Lubimov, Izv. Vuzov. Chernaja Metallurgija **9**, 136 (1963)
19. F. Lihl, A. Schwaiger, Z. Metallkde **58**, 777 (1967)
20. R. Elliot, *Eutectic Solidification Processing* (Butterworths, London, 1983)
21. B. Xiufang, W. Weimin, Y. Shujuan, Q. Jingyu, Sci. Technol. Adv. Mat. **2**, 19 (2001)
22. S. Mudry, A. Korolyshyn, I. Shtablavyi, J. Phys., Conf. Series **98**, 012016 (2008)
23. R. Brandt, G. Neuer, Int. J. Thermophys. **28**, 1429 (2007)
24. F. Mott, E. Davis, *Electron Processes in Non-crystalline Materials* (Clarendon Press, Oxford, 1979)
25. J. Friedel, Nuovo Cimento, Suppl. **7**, 287 (1958)
26. T. N. Faber, J.M. Ziman, Phil. Mag. **11**, 153 (1965)
27. J.M. Ziman, *The Physics of Metals*, chs. 5,6. (University Press, Cambridge, 1969)